STRAIN GAUGE IMPLEMENTATION FOR A Nb_3Sn SUPERCONDUCTING MULTIPOLE WIGGLER DEVELOPED IN KEK PHOTON FACTORY

S. Nishi*
The Graduate University for Advanced Studies, SOKENDAI, Hayama, Japan
C. Mitsuda, K. Suzuki, H. Saito, S. Shinohara, T. Nogami, T. Ogitsu, K. Tsuchiya, S. Eguchi
High Energy Accelerator Research Organization (KEK), Tsukuba, Japan
K. Saito, M. Yoshikawa, S. Ito, S. Yokoyama
Japan Superconductor Technology, Inc. (JASTEC), Hyogo, Japan

Abstract

KEK Photon Factory is developing a Nb_3Sn superconducting multipole wiggler for a next generation light source ring. Following the Unit 1 [1], we conducted an excitation test of the Unit 2 at the current density of 378 A/mm^2. In this test, one of the purposes is to evaluate a new strain measurement system that was first introduced into the Unit 2. Multiple strain gauges were attached at positions determined by FEM simulation. We also compared simulation and measured results to assess the FEM model. In the future, we plan to conduct excitation tests at the target current density of 1000 A/mm^2. In the test, a strain-monitoring system will be implemented to the quench detection. We report the Unit 2 test results and progress toward the next excitation test.

INTRODUCTION

In KEK Photon Factory, Nb_3Sn superconducting multipole wiggler (SC-MPW) units are being developed as part of the technology development toward next generation light source ring. The main design parameters of the SC-MPW test-coil unit are listed in Table 1.The full-length device is designed to have 14 poles, corresponding to 7 wiggler periods. At present, two short-model SC-MPW units with 3 poles and 1.5 wiggler periods are being fabricated in order to identify fabrication issues prior to the construction of the full-length device. In this paper, the test-coil unit refers to a single unit, whereas the complete device consists of two facing units. The 300 A excitation test is the first test after heat treatment and impregnation. The test was launched as a validation program whose goal is to check conformity of the coils as well as commissioning of the quench protection, DAQ, strain-monitoring and temperature-monitoring system. Because the SC-MPW uses strain-sensitive Nb_3Sn conductor, strain monitoring during cool-down and excitation is a central issue at this stage. In this paper, we present the results of the excitation test of the second test-coil unit and the strain measurements, and discuss future prospects.

DETERMINATION OF STRAIN MONITORING POINTS

The strain to be monitored is the coil strain, $\varepsilon_{\mathrm{coil}}$, which includes thermal strain during cool-down and Lorentz-force-induced strain during excitation. During cool-down, an apparent strain, $\varepsilon_{\mathrm{apparent},T}$, arises from the temperature dependence of the gauge resistance and the differential thermal contraction between the strain gauge and the coil. During excitation, an additional apparent strain, $\varepsilon_{\mathrm{apparent},B}$, arises from magnetoresistance. Taking tensile strain as positive, the strain-gauge reading attached to the coil is written as $\varepsilon_{\mathrm{SG}} = \varepsilon_{\mathrm{coil}} + \varepsilon_{\mathrm{apparent},T} + \varepsilon_{\mathrm{apparent},B}$. Here, $\varepsilon_{\mathrm{coil}}$ is decomposed into the free thermal strain, $\varepsilon_{\mathrm{free}}$, and the mechanical strain, $\varepsilon_{\mathrm{mech}}$. In the present analysis, $\varepsilon_{\mathrm{mech}}$ is treated separately for cool-down and excitation. The free thermal strain is the strain integrated as the coil cools from room temperature to the operating temperature (4.2 K), based on the linear thermal expansion coefficient of the coil, α_{coil}. The $\varepsilon_{\mathrm{mech(cooldown)}}$ denotes the mechanical strain induced during cool-down by coil constraints and by differential thermal contraction between the coil and the support structure, whereas $\Delta\varepsilon_{\mathrm{mech(excitation)}}$ denotes the mechanical strain increment during excitation, including the contributions of Lorentz forces and the coil support structure. Accordingly, during cool-down, $\varepsilon_{\mathrm{SG(cooldown)}}$ is given by the sum of $\varepsilon_{\mathrm{free}}$, $\varepsilon_{\mathrm{mech(cooldown)}}$, and $\varepsilon_{\mathrm{apparent},T}$. Thus, the coil strain during cool-down is obtained by correcting the measured value for $\varepsilon_{\mathrm{apparent},T}$. For excitation, the strain increment is evaluated with respect to the state after cool-down and before excitation. The strain-gauge reading increment during excitation, $\Delta\varepsilon_{\mathrm{SG(excitation)}}$, is then given by the sum of $\Delta\varepsilon_{\mathrm{mech(excitation)}}$ and $\Delta\varepsilon_{\mathrm{apparent},B}$. The mechanical strain increment during excitation is obtained by correcting the measured increment for $\Delta\varepsilon_{\mathrm{apparent},B}$. Based on this formulation, compensation

Table 1: Main Design Parameter of the SC-MPW Test Coil Unit

Item	Specification
operating temperature	4.2 K
superconducting wire	Nb_3Sn
fabrication process	bronze process
Wire dia. (insulation)	1.2 mm (1.36 mm)
Copper ratio (Cu/Cu+Non-Cu)	0.3 ±0.1
current	792 A (1000 A/mm^2)
number of turns	493 turns
magnetic field on the beam axis	> 2 T
magnetic period length	80 mm
pole gap	> 30 mm

* snishi@post.kek.jp

gauges were installed in addition to the gauges used to measure $\varepsilon_{\mathrm{coil}}$. To determine the strain-monitoring locations for $\varepsilon_{\mathrm{coil}}$, an FEM simulation was performed using ANSYS. The magnetic-field distribution in a single coil unit is summarized in Fig. 1.

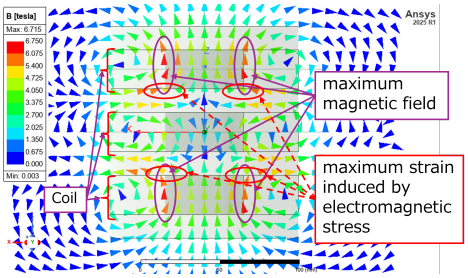

Figure 1: Magnetic field in a single coil unit at 792 A.

The highest magnetic field 6.7 T occurs in the region between the bobbins and upper or lower coils. The location of the maximum strain also corresponds to this region. It is not possible to directly instrument the location at which the maximum strain is generated. We therefore adopted an indirect approach in which strain gauges were mounted on the coil surface; the simulation model was validated by comparing the measured surface strain with the simulated values, and the internal strain was then estimated using the validated model. The monitoring layout is summarized in Fig. 2. SG 1 and SG 2 were used to measure $\varepsilon_{\mathrm{coil}}$, whereas SG 3 and SG 5 were used to correct $\varepsilon_{\mathrm{apparent},T}$ and $\Delta\varepsilon_{\mathrm{apparent},B}$, respectively. SG 4 was attached to an impregnation-material sample for comparison with the simulation. Self-temperature-compensated three-wire strain gauges (KYOWA, KFLB-2-120-C1-23 F3M3) and a UCAM60B static strain meter were used at a sampling rate of 1 Hz.

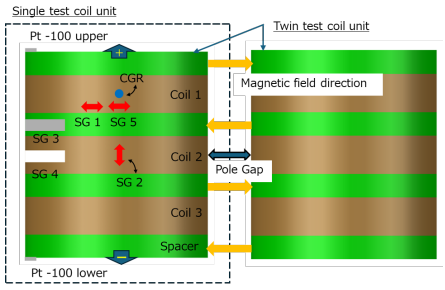

Figure 2: Strain-monitoring layout and sensor assignment.

EXCITATION TEST OF UNIT 2

The Unit 2 excitation test was carried out at JASTEC. The current and voltage traces for the five 300 A excitation tests are summarized in Fig. 3. Five runs reached 300 A without coil quench; only the third run was interrupted by a current-lead quench due to a low liquid-helium level.

STRAIN MEASUREMENT RESULTS DURING COOL-DOWN

Both the measurement and the simulation involve uncertainties. The measured values are affected by strain-gauge

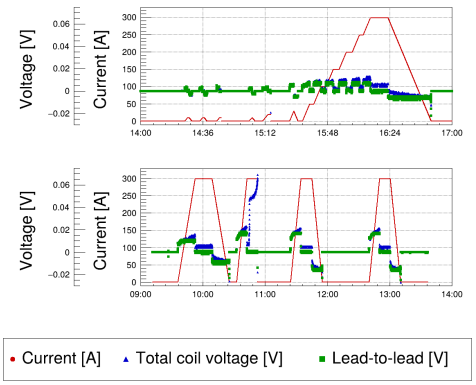

Figure 3: Current, total coil voltage, and current-lead voltage during the five 300 A excitation tests.

installation errors, transient responses after liquid-helium filling, and the location mismatch between the temperature monitoring points and the strain monitoring points, whereas material properties used in the simulation are based on literature values and the coil model is simplified. We therefore compare not only the absolute strain values but also the strain changes before and after cool-down and excitation. The strain and temperature histories during cool-down are summarized in Fig. 4. For the correction of $\varepsilon_{\mathrm{apparent},T}$ in Eq. (1), the plateau value after immersion in liquid helium was used, and $\Delta\varepsilon_{\mathrm{Al}}$ corresponds to SG 3 in Fig. 2. $E_{\mathrm{Al}}^{\mathrm{ref}}$ denotes the reference strain of aluminum from room temperature to 4.2 K.

$$\varepsilon_{\mathrm{apparent},T} = \Delta\varepsilon_{\mathrm{Al}}(\text{room temp} \rightarrow 4.2\,\mathrm{K}) - E_{\mathrm{Al}}^{\mathrm{ref}} \quad (1)$$

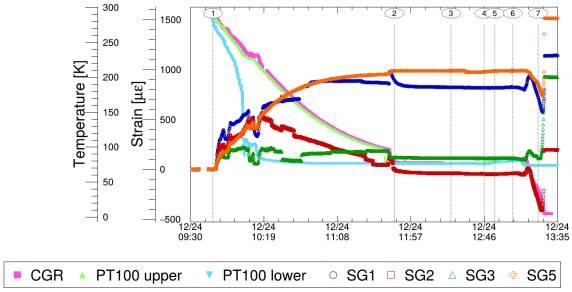

Figure 4: The numbered markers correspond to the following cooling steps: 1, start of LN_2 cooling; 2, completion of LN_2 pre-cooling; 3, start of N_2 removal; 4, LN_2 replenishment to the shield and gas purge after N_2 removal; 5, completion of LN_2 replenishment to the shield; 6, start of helium purge; and 7, confirmation of the superconducting transition.

The coil strain was corrected for the temperature-induced apparent strain, $\varepsilon_{\mathrm{apparent},T}$, using Eq. (2).

$$E_{\mathrm{thermal}} = \Delta\varepsilon_{\mathrm{coil}}(\text{room temp} \rightarrow 4.2\,\mathrm{K}) - \varepsilon_{\mathrm{apparent},T} \quad (2)$$

Using Eqs. (1) and (2), SG 1 and SG 2 were evaluated as -3920 ± 5.0 με and -4857 ± 4.0 με, respectively. For

the simulation, because the material properties of the coil and the volume fractions of Nb_3Sn and the impregnation material are not well defined, the coil was modeled as a composite. The effective properties were estimated from the properties of Nb_3Sn and the datasheet values of the impregnation material [2]. The corresponding simulation results before and after cooling are summarized in Fig. 5. SG 1 is consistent with an Nb_3Sn-to-impregnation-material volume ratio of approximately 90:10, whereas SG 2 is consistent with approximately 85:15. This difference is likely attributable to the anisotropy of the Nb_3Sn conductor, which was not included in the model, and to the uncertainty in the conductor filling factor [3].

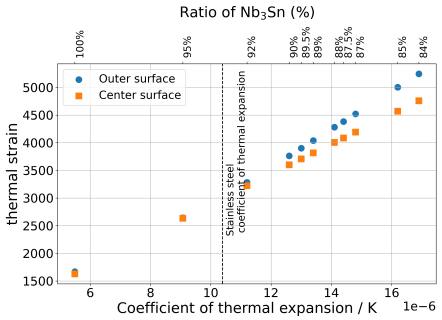

Figure 5: Simulated strain distribution before and after cooling from 293 K to 4.2 K.

STRAIN MEASUREMENT RESULTS DURING EXCITATION

The coil-surface strain at SG 1 and the magnetoresistance-induced apparent strain measured by the compensation gauge are plotted together in Fig. 6.

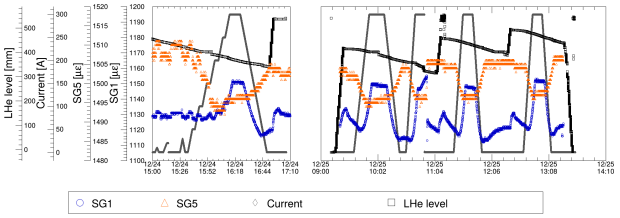

Figure 6: Coil-surface strain at SG 1 and magnetoresistance-induced apparent strain measured by SG 5.

At SG 1, the strain increased with current, whereas the compensation signal decreased. Simulations give a field of about 1 T at the compensation gauge at 300 A, where Ni–Cr gauges can show a negative apparent response [4].The strain was corrected using Eq. (3). Because transient responses after liquid-helium filling and baseline shifts after ramp-down prevented the use of a single absolute reference, the strain was evaluated as a cycle-specific increment. The values before excitation, during the current plateau, and after ramp-down were then used to determine the increment and its uncertainty.

$$\Delta\varepsilon_{\mathrm{mech(excitation)}} = \Delta\varepsilon_{\mathrm{SG(excitation)}} - \Delta\varepsilon_{\mathrm{apparent},B} \pm \sqrt{\sigma^2_{\mathrm{SG(excitation)}} + \sigma^2_{\mathrm{apparent},B}} \quad (3)$$

$$\Delta\varepsilon_{\mathrm{SG(excitation)}} = \varepsilon_{\mathrm{plateau}} - \varepsilon_{\mathrm{before(after)\ excitation}} \pm \sqrt{\sigma^2_{\mathrm{plateau}} + \sigma^2_{\mathrm{before(after)\ excitation}}} \quad (4)$$

As a result, it was found that excitation up to 300 A produced 37 ± 1 με strain due to Lorentz-force-induced stress.The measured strain increment is compared with the simulation results. The results are summarized in Table 2. Condition 1 uses the properties of Nb_3Sn only. For Conditions 2 and 3, a 9:1 volume ratio of Nb_3Sn to impregnation material was assumed for the orthocyclic-wound coil.

Table 2: Simulation Conditions and Coil Surface Strain

Current [A]	**Young module** K [GPa]	α/K [K^{-1}]	**strain** [με]
300	120	5.49×10^{-6}	21
300	108.4	1.26×10^{-5}	16
300	81.4	1.26×10^{-5}	18

Comparison with the simulation results shows a discrepancy of approximately 15~20 με. Possible reasons for this discrepancy include the fact that the anisotropy in the coefficient of linear thermal expansion and Young's modulus of the Nb_3Sn conductor was not taken into account, that the material properties of the sample measured in this study were not incorporated, and that the coil was treated as a homogeneous composite material. Therefore, a more realistic model of the actual coil, which reproduces the winding structure is currently being developed.

CONCLUSION

The 300 A excitation test of Unit 2 confirmed coil integrity and demonstrated that the coil-surface strain can be resolved during excitation. The remaining discrepancy between the measured strain and the simulation indicates that the analysis procedure and the material model must be refined before the 792 A test. In preparation for future high-current tests, the strain-monitoring system will be extended to dynamic measurements so that rapid strain changes associated with quench events can be detected.

ACKNOWLEDGEMENTS

This work was supported by JST SPRING, Japan Grant Number JPMJSP2104.

REFERENCES

[1] C. Mitsuda *et al.*, "Test coil-unit fabrication of Nb3Sn superconducting multipole wiggler for next generation light source in KEK-PF", in *Proc. IPAC'25*, Taipei, Taiwan, Jun. 2025, pp. 1851–1854. doi:10.18429/JACoW-IPAC2025-WEPB050

[2] K. P. Weiss, A. Nyilas, M. Thoener, and B. Seeber, "Proof strength behavior of Nb_3Sn bronze route wires between 300 and 4 K", *AIP Conf. Proc.*, vol. 986, no. 1, pp. 293–300, Mar. 2008. doi:10.1063/1.2900359

[3] S. Höll, M. Guinchard, S. Izquierdo Bermudez, and Ó. Sacristán De Frutos, "Study on the thermal contraction behavior of state-of-the-art Nb_3Sn superconducting magnet coils in the longitudinal, azimuthal, and radial direction", *IEEE Trans. Appl. Supercond.*, vol. 34, no. 5, p. 4003006, Aug. 2024. doi:10.1109/TASC.2024.3356475

[4] H. S. Freynik Jr., D. R. Roach, D. W. Deis, and D. G. Hirzel, "Nickel-chromium strain gages for cryogenic stress analysis of superconducting structures in high magnetic fields", Lawrence Livermore Laboratory, Livermore, CA, USA, Rep. UCRL-79726, CONF-771029-101, 1977.